BBA - Molecular Basis of Disease 1871 (2025) 167524

Contents lists available at ScienceDirect

BBA - Molecular Basis of Disease

journal homepage: www.elsevier.com/locate/bbadis

Monocyte and macrophage profiles in patients with inherited long-chain fatty acid oxidation disorders

Sanne G.S. Verberk [a,b], Nico Hahn [a], Daan Heister [a], Jorien Haverkamp [c], Khya S. Snelder [c], Kyra E. de Goede [a], Friederieke S. Gorki [a,d], Jerome J.A. Hendriks [b], Riekelt H. Houtkooper [e,f], Gepke Visser [g], Barbara Sjouke [c,h], Mirjam Langeveld [c], Jan Van den Bossche [a,*]

[a] Department of Molecular Cell Biology and Immunology, Amsterdam Cardiovascular Sciences, Amsterdam Gastroenterology Endocrinology Metabolism, Amsterdam Institute for Infection and Immunity, Cancer Centre Amsterdam, Amsterdam UMC, Vrije Universiteit Amsterdam, Amsterdam, the Netherlands
[b] Department of Immunology and Infection, Biomedical Research Institute, Hasselt University, Diepenbeek, Belgium
[c] Department Endocrinology and Metabolism, Amsterdam UMC, University of Amsterdam, Amsterdam, the Netherlands
[d] Institute of Innate Immunity, University Hospital Bonn, University of Bonn, Bonn 53127, Germany
[e] Laboratory Genetic Metabolic Diseases, Amsterdam Gastroenterology Endocrinology Metabolism, Amsterdam Cardiovascular Sciences, Amsterdam UMC, University of Amsterdam, Amsterdam, the Netherlands
[f] Emma Center for Personalized Medicine, Amsterdam UMC, Amsterdam, the Netherlands
[g] Emma Children's Hospital, Department of Pediatrics, Division of Metabolic Diseases, Amsterdam Gastroenterology Endocrinology and Metabolism, Amsterdam UMC, location University of Amsterdam, Amsterdam, the Netherlands
[h] Department of Internal Medicine, Radboud University Medical Centre, Nijmegen, the Netherlands

ARTICLE INFO

Keywords:
Fatty acid oxidation disorders
Macrophages
Inflammation
Immunophenotyping
Immunometabolism

ABSTRACT

Patients with inherited disorders of the long-chain fatty acid oxidation (lcFAO) machinery present with a heterogeneous profile of disease manifestations and aggravation of symptoms is often triggered by inflammatory activation. Monocytes and macrophages are innate immune cells that play a major role in the onset and resolution of inflammation. These cells undergo metabolic rewiring upon activation including the regulation of the FAO rate. The rewiring of FAO and the effect of lcFAO disorders (lcFAOD) on human monocyte and macrophage phenotype and function remain largely unknown. Here, we performed extensive phenotyping of circulating monocytes and analyzed plasma cytokine levels in 11 lcFAOD patients and 11 matched control subjects. In patients with lcFAOD, we observed induced plasma levels of the inflammatory cytokines IL-1β and IL-6, and enhanced CD206 and CD62L surface marker expression in circulating monocyte subsets. To mimic the most common lcFAOD very-long-chain acyl-CoA dehydrogenase disorder (VLCADD), we used siRNA-mediated knockdown of the *ACADVL* gene (encoding VLCAD) in macrophages derived from healthy volunteers. Hereby, we found that siVLCAD affected IL-4-induced alternative macrophage activation while leaving LPS responses and cellular metabolism intact. In the same line, monocyte-derived macrophages from lcFAOD patients had elevated levels of the IL-4-induced alternative macrophage markers CD206 and CD200R. Still, they did not show major metabolic defects or changes in the LPS-induced inflammatory response. Our results indicate that monocytes and macrophages from lcFAOD patients present no major inflammatory or metabolic differences and show that IL-4-induced surface markers are intertwined with lcFAO in human macrophages.

1. Introduction

Fatty acid oxidation (FAO) is an important metabolic pathway that provides energy *via* the breakdown of short-, medium-, and long-chain fatty acids (FAs) in the mitochondria. Mutations in genes encoding enzymes involved in the FAO machinery can reduce the ability to metabolize long-chain FAs, resulting in altered energy homeostasis and the accumulation of long-chain acylcarnitines [1]. Patients with defective long-chain FAO (lcFAOD) present with a heterogeneous range of symptoms that mainly arise in catabolic situations like fasting, illness, or endurance exercise [2]. Common symptoms include hypoglycemia, liver dysfunction, cardiomyopathy, and rhabdomyolysis [3,4]. While these

* Corresponding author.
E-mail address: j.vandenbossche@amsterdamumc.nl (J. Van den Bossche).

https://doi.org/10.1016/j.bbadis.2024.167524
Received 9 April 2024; Received in revised form 17 September 2024; Accepted 17 September 2024
Available online 20 September 2024

symptoms do not directly indicate activation of immune responses, but the accumulation of bio-active acylcarnitines and rhabdomyolysis can both be linked to inflammatory activation [5,6].

The accumulation of long-chain acylcarnitines can provoke inflammatory responses in macrophages *via* MyD88-signaling [7]. Additionally, the rapid destruction of muscle tissue during rhabdomyolysis observed in lcFAOD, can signal to the immune system to induce clearance of damaged cells by phagocytosing macrophages. This highlights the role of external (metabolic) signaling in dictating macrophage activation in lcFAOD. In line with this, inflammatory activation has been reported in individuals deficient in very long-chain acyl-CoA dehydrogenase (VLCAD, encoded by *ACADVL*), long-chain 3-hydroxy-acyl-CoA dehydrogenase (LCHAD), or carnitine palmitoyltransferase 2 (CPT2) in homeostatic non-symptomatic conditions and in times of metabolic decompensation [5,6]. In parallel to being regulated by external signaling, macrophage activation is also tightly controlled by intracellular metabolic rewiring, including altered fatty acid metabolism [8,9].

Due to their diverse roles in both initiating and resolving inflammation, macrophages undergo metabolic rewiring to meet their cellular demands [8,10]. Alternative macrophage activation with IL-4 *in vitro* increases FAO flux [11,12]. However, FAO was found to be dispensable for IL-4-induced alternative activation, as evidenced by experiments utilizing specific knockout mice and by the application of relevant concentrations of CPT1-inhibitor etomoxir [10,11,13,14]. Conversely, inflammatory activation of mouse macrophages with lipopolysaccharide (LPS) *in vitro* increases the glycolytic flux and downregulates mitochondrial activity and FAO [8], which is also apparent in monocytes, the precursor cells of macrophages [15]. However, the initial view that glycolysis drives inflammation while FAO is anti-inflammatory, is oversimplified and outdated [16]. As such, in glucose-deprived conditions, LPS-induced activation of monocytes is compensated by also increasing FAO flux [15]. Furthermore, FAO contributes to the activation of the NLRP3-inflammasome [17,18] and plays a stimulating role in atherosclerosis progression in lipid-rich conditions [19,20]. Despite its involvement in various processes during inflammation and resolution, the incidence of inflammatory disorders such as atherosclerosis in patients with lcFAO disorders has not been studied.

There are apparent contradictions regarding the role of FAO in macrophage inflammatory or alternative activation, and most of our current knowledge is derived from studies in mouse models. Therefore, we here aimed to decipher how genetic interruptions in lcFAO alter systemic inflammation, leukocyte and macrophage function, and cellular metabolism. Additionally, we profiled monocytes and baseline inflammatory signaling in lcFAOD patients to further study excessive inflammation reported before. Hereto, we collected blood from lcFAOD patients and time-, sex- and age-matched healthy controls in homeostatic non-symptomatic conditions. We demonstrate with flow cytometry that monocytes from lcFAOD patients are phenotypically slightly different from controls, and that there is a minor induction of plasma IL-6 and IL-1β levels. Additionally, we observed that in human monocyte-derived macrophages (hMDM) from lcFAOD, as well as in healthy control hMDMs with siRNA-mediated knockdown of *ACADVL,* IL-4-induced alternative macrophage activation is altered, whilst LPS-induced inflammatory responses remain unchanged. Together with previous findings on increased inflammatory signaling in lcFAOD patients [5,6], our study reveals that lcFAOD minimally impacts basal inflammatory markers in patients. Moreover, our study showed that in human macrophages, a deficiency of FAO causes subtle alterations in IL-4-induced macrophage activation and not in LPS-stimulated macrophages.

2. Results

2.1. LcFAOD patients do not present major inflammatory differences in monocytes at baseline or after LPS stimulation of whole blood

Given that a genetic deficiency in lcFAO affects all cells in the body [21], and since cellular metabolism regulates immune cell activation, we determined immunological parameters in blood from 11 lcFAOD patients who visited the outpatient metabolic clinic over 4 years and compared their results to 11 age- and sex-matched healthy controls that were analyzed simultaneously (Table 1). All patients were diagnosed with a genetic defect in lcFAO but differed in their affected genes, the underlying mutation, and enzyme activity in lymphocytes and fibroblasts (Table 1).

Generally, monocytes can be classified as classical ($CD14^{++}CD16^{-}$), intermediate ($CD14^{+}CD16^{+}$), and non-classical monocytes ($CD14^{-}CD16^{+}$) and altered abundance of these subsets is often associated with inflammatory diseases [22,23]. Each subset has its specific pattern of surface marker expression, which we assessed by flow cytometry. LcFAOD patients did not have altered total leukocyte or monocyte counts (Fig. 1A, Supplementary Fig. 1A) and the abundance of monocyte subsets was similar in control and lcFAOD patients (Fig. 1B). Although the surface levels of most activation markers were identical in both groups, non-classical monocytes from lcFAOD patients showed 3-fold enhanced CD206 expression, and their intermediate monocytes displayed 1.3-fold enhanced CD11c surface levels as compared to healthy controls (Fig. 1C, Supplementary Fig. 1B). Plasma IL-6 and IL-1β levels were slightly elevated in lcFAOD patients by 2.5- and 2.7-fold, respectively (Fig. 1D), while all other cytokines were unaltered. Yet, it should be noted that the observed levels were still within a range previously reported in healthy control subjects and as such there is no evidence that lcFAOD patients have relevant systemic inflammatory signaling defects in a stable outpatient setting [24–26].

Despite that cellular stress may initiate the typical accumulation of acylcarnitines and thus inflammatory activation in lcFAOD patients, *ex vivo* induction of cellular stress in whole blood by adding LPS provoked similar inflammatory responses in controls and patients (Fig. 1E). Together, these findings indicate that lcFAOD patients show a modest difference in immune status in homeostatic conditions compared to healthy controls, and mount a normal inflammatory response upon activation.

2.2. The lcFAO-machinery is regulated by macrophage inflammatory and alternative activation

Stimulation with either LPS or IL-4 differentially rewires macrophage metabolism including altering the rate of FAO [12,27]. In line with this, human monocyte-derived macrophages (hMDMs) stimulated with LPS displayed enhanced oxygen consumption rates (OCR). Since these cells were not affected by the CPT1-inhibitor etomoxir, LPS-induced enhanced OCR was mostly independently of FAO, (Fig. 2A). Additionally, stimulation of hMDMs with LPS or IL-4 affected the expression of genes involved in lcFAO. Indeed, IL-4 elevated the expression of *ACADVL* and *SLC25A20*, while LPS decreased the expression *ACADM* and *CD36* in healthy controls (Fig. 2A). These findings confirm existing literature describing that human LPS-stimulated macrophages barely use FAO to fuel their metabolic needs [9].

Given the systemic inflammatory signaling reported in VLCADD patients [5], we investigated the effect of ±60 % *ACADVL* knockdown on human macrophage function (Supplementary Fig. 2). Since increased FAO can reduce foam cell formation [28], we first checked whether *ACADVL* knockdown affected foam cell formation. Loading of si*ACADVL* hMDMs with a 1:2 ratio of oleate (18:1) over palmitate (16:0) resulted in intracellular lipid accumulation, to a similar extent as control hMDMs (Fig. 3A).

Additionally, metabolic activity, as determined by MTT assay and extracellular flux analysis, of si*ACADVL* low-lipid and foamy hMDMs responded similarly to LPS as scRNA-hMDMs (Fig. 3B-D). While increasing mitochondrial activity in FA-loaded hMDMs, LPS-treatment reduced FAO dependency regardless of *ACADVL* knockdown, suggesting that LPS can modulate metabolism in low-lipid and foamy cells independently of lcFAO. In conclusion, siRNA-mediated knockdown of

Table 1
Genetic defects, enzyme activity, CK serum values, and characteristics of controls and lcFAOD patients. CK: Creatine kinase, U.D.; undetermined, N.A.; not applicable, M/F; Male/Female, [1]OMIM 201,475, [2]OMIM 609,015, [3]OMIM 255,110, [4]OMIM 609,016, [5]OMIM 600,528, *Not detectable. Reference values enzyme activity lymphocytes (nmol/(min.mg protein)): VLCAD 1.84–4.80, LCHAD 22–74, LCKAT 23–43, CPTII 7.7–11.7. Reference values enzyme activity fibroblasts (nmol/(min.mg protein)): LCHAD 34–114, LCKAT 58–110, VLCAD 8.8–19.6 (subject 4) or 1.48–5.24 (subject 10).

	lcFAOD									Matched healthy control		
	Disorder	Gene mutation	Enzyme activity (% of reference values)		Average CK (U/L) outpatient visit	Max CK (U/L)	Sex	Age (y)	BMI (kg/m^2)	Sex	Age (y)	BMI (kg/m^2)
			Lymphocytes	Fibroblasts								
1	VLCADD[1]	In *ACADVL*: c.520G > A (p.V174M) and c.833-835delAAG (p.K278del)	VLCAD: 8.8–22.2 %	U.D.	281 (77–697)	U.D.	M	49	28.3	M	42	20.8
2	MTPD[2]	In *HADHB*: c.209 + 1G > C (splicing defect) and c.980 T > C (p.Leu327Leu) mutation	LCHAD: 8.1–27.2 % LCKAT: 4.6–8.7 %	LCHAD: 10.5–35.3 % LCKAT: 5.5–10.3 %	305 (122–1286)	44,664	F	25	24.8	F	31	23.5
3	CPTIID[3]	In *CPT2*: Homozygous c.338C > T (p.Ser13Leu)	U.D.	U.D.	283 (93–609)	55,080	M	22	28.0	M	27	25.4
4	VLCADD[1]	In *ACADVL*: c.664G > A (p.G222R) and c.1512G > C (p.E504D)	VLCAD: 4.3–6.5 %	VLCAD: 1.5–3.4 %	90 (82–97)	U.D.	M	57	24.0	M	59	24.8
5	LCHADD[4]	In *HADHA*: Homozygous c.1528G > C (p.Glu510Gln)	LCHAD: <2.7–9.1 % * LCKAT: 25.6–47.8 %	LCHAD: 5.3–17.6 % LCKAT: 61.8–117.2 %	90 (84–97)	7493	F	40	24.7	F	44	20.2
6	LCHADD[4]	In *HADHA*: c.1528G > C (p.Glu510Gln) and c.1678C > T (p.Arg560*)	U.D.	LCHAD: 4.4–14.7 % LCKAT: 23.6–44.8 %	72 (37–151)	U.D.	F	33	25.8	F	27	20.5
7	CPTIID[3]	In *CPT2*: Homyzogous c.149C > A (p.Pro50His)	CPTII: 17.9–27,3 %	U.D.	448 (104–1555)	35,000	M	43	27.8	M	38	23.1
8	MTPD[2]	In *HADHA*: c.556C > G (p.Gln186Glu) and c.1392 + 1G > A	LCHAD: <2.7–9.1 % * LCKAT: 2.3–4.3 %	LCHAD: 4.4–14.7 % LCKAT: 1.8–3.4 %	245 (107–385)	19,731	M	24	22.6	M	26	22.8
9	MTPD[2]	In *HADHA*: c.556C > G (p.Gln186Glu) and c.1392 + 1G > A	LCHAD: 13.5–45.5 % LCKAT: <11.6–23 %	LCHAD: 4.4–14.7 % LCKAT: 1.8–3.4 %	491 (117–871)	295,460	M	26	27.2	M	29	23.5
10	VLCADD[1]	In *ACADVL*: c.541dupC (p.His181ProfsX72) and c.1072 A > G (p.Lys358Glu)	VLCAD: 4.2–10.9 %	VLCAD: 6.1–21.6 %	1350 (142–5498)	213,398	M	29	25.7	M	26	22.4
11	CPTID[5]	In *CPT1A*: Homozygous c.657_692del (p.Trp219_Tyr231delinsCys)	U.D.	CPTI: 6 %	37 (35–37)	N.A.	F	25	30.4	F	22	19.9
						Average	M6: F5	33.9	26.3	M6: F5	33.7	22.4
						±SEM		*3.4*	*0.6*		*3.2*	*0.5*

ACADVL does not elicit metabolic differences in hMDM.

Lastly, to determine macrophage polarization after *ACADVL*-knockdown we stimulated cells with LPS and IL-4 and measured typical LPS- and IL-4-induced responses. si*ACADVL* did not alter LPS-induced IL-6 secretion or *IL6* and *TNF* gene expression (Fig. 3E, F) nor did it change the expression of LPS-induced surface markers (Fig. 3F, G). On the other hand, the IL-4-induced expression of CD273 was decreased by 0.8-fold, and CD206 was 1.2-fold increased in si*ACADVL* macrophages (Fig. 3F, G), indicating that VLCAD plays a multifaceted role in the phenotype of IL-4-induced macrophages.

2.3. Macrophages from lcFAOD-patients increase IL-4-induced surface markers without affecting core metabolic pathways

We have previously shown that long-term genetic metabolic disruptions can induce advanced metabolic rewiring as opposed to short-term inhibition of a metabolic pathway by small-molecules or siRNA [29,30]. To study whether long-term genetic disruptions in lcFAO affect macrophage metabolism, we cultured hMDMs from lcFAOD patients and controls and determined their metabolic activity. Differentiation and maturation were not significantly altered in patient hMDMs compared to control hMDMs (Supplementary Fig. 3). Extracellular flux analysis on these macrophages presented no alterations in basal mitochondrial respiration and basal glycolysis (Fig. 4A-C). Additionally, mito stress test parameters did not reveal metabolic remodeling in macrophages of lcFAOD patients (Fig. 4D, E). We analyzed FAO dependency by blocking mitochondrial FA import using etomoxir, and found no significant difference between lcFAOD or control hMDMs (Fig. 4F), suggesting that there is residual FAO dependency in hMDMs from lcFAOD patients.

Aligning with the altered IL-4-induced surface marker expression following *ACADVL* knockdown (Fig. 3G), the expression levels of CD206 and CD200R were 1.3- and 1.7-fold elevated, respectively, in IL-4-stimulated macrophages from lcFAOD patients, whilst LPS-induced cytokine secretion or CD80, CD40, and CCR2 surface expression remained unaffected in comparison to controls (Fig. 4G, H). These results indicate that lcFAOD macrophages are more capable of adopting IL-4-induced properties.

3. Discussion

Patients with lcFAO defects are previously reported to have a modest increase in inflammatory signaling [5,6], substantiating the potential link between lcFAO and inflammation. Macrophages intricately regulate cellular metabolism, including lcFAO, to meet the energy demands of

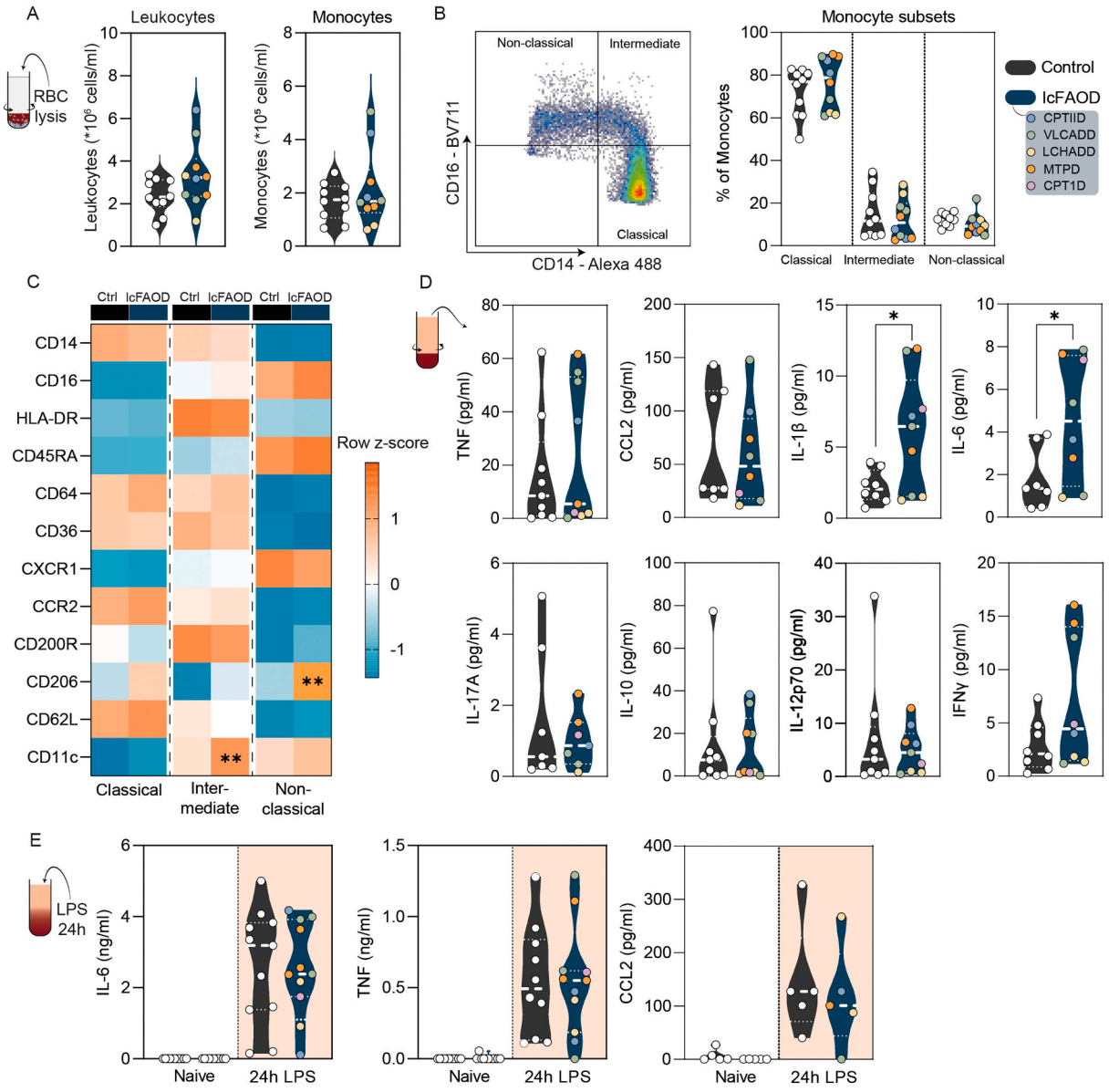

Fig. 1. lcFAOD patients present slightly altered monocyte phenotypes and enhanced plasma cytokines, but similar *ex vivo* inflammatory LPS responses. A) Absolute leukocyte counts after red blood cell (RBC) lysis and monocyte counts as determined by the gating strategy depicted in Fig. S1A. B) Percentage of monocyte subsets classified as classical ($CD14^{++}CD16^{-}$), intermediate ($CD14^{++}CD16^{+}$), and non-classical ($CD14^{+}CD16^{+}$). C) Surface marker expression on monocyte subsets from controls and lcFAOD patients presented as row z-scores from ΔMFI (median fluorescent $intensity_{sample}$-median fluorescent $intensity_{FMO}$). D) Cytokine levels in plasma from controls and lcFAOD patients. E) Cytokine levels after whole blood stimulation with 100 ng/ml LPS for 24 h. Data are shown as median and quartile range (A, B, D, E).). Each dot represents a control or patient sample ($n = 10$ controls, 10 patients (B, C, D), $n = 11$ controls, 11 patients (E)). Data is shown as row z-score determined from average ΔMFI for each marker (n = 10 controls, 10 patients) (C). $^{*}P < 0.05$ or $^{**}P < 0.01$ by one-way ANOVA with Sidak's correction for multiple comparisons (C) or by unpaired two-tailed *t*-test (D).

various activation states. Enhanced lcFAO is generally considered to be associated with an alternatively activated or IL-4-induced macrophage phenotype [10,13]. However, studies using genetic modulation of FAO revealed that an anti-inflammatory macrophage phenotype was not dependent on β-oxidation [13,31]. In this study, we examined the complex interplay of lcFAO and inflammation by studying the effect of lcFAOD on monocyte phenotype in steady-state conditions, and on macrophage activation and metabolism.

We found that monocytes from lcFAOD patients showed modest alterations in CD11c and CD206 surface levels. Additionally, in line with previous reports, we confirmed a minor increase in systemic inflammatory cytokine levels in lcFAOD patients. Furthermore, macrophages with *ACADVL* knockdown and macrophages from lcFAOD showed altered IL-4-induced cell surface markers without changes in basal metabolic pathways or LPS-induced inflammatory activation. As such, we demonstrate that lcFAO plays a role in macrophage IL-4-induced activation *in vitro* and slightly affects monocyte phenotypes and systemic inflammatory signaling in lcFAOD patients.

Two studies on lcFAOD, focusing primarily on VLCAD and MTP deficiencies, revealed a notable increase in multiple inflammatory cytokines in both plasma and circulating immune cells [5,6]. Vallejo et al. compared 18 mainly pediatric VLCADD patients to 9 controls, showing elevated pro- and anti-inflammatory cytokines during outpatient visits and admissions due to rhabdomyolysis [5]. McCoin et al. studied 12 mainly pediatric LCHADD patients in an outpatient setting compared to 12 sex and age matched control subjects, showing a modest elevation in plasma levels of some pro-inflammatory cytokines [6]. Similarly, we also observed a modest elevation in IL-6 and IL-1β levels, but not in other

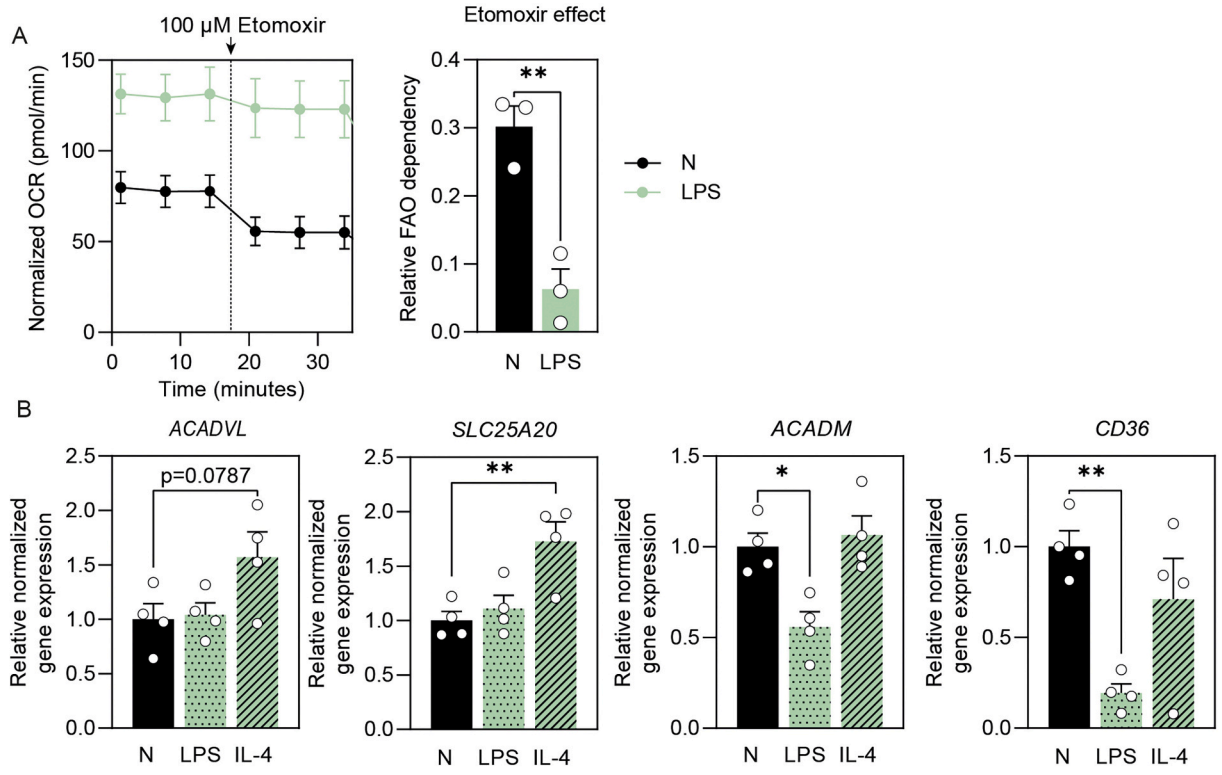

Fig. 2. LPS- and IL-4-stimulation regulates long-chain FAO in human macrophages. A) Expression of genes involved in long-chain FAO in human MDMs from healthy donors in response to LPS or IL-4. B) Relative OCR dependent on FAO in naïve and LPS-stimulated healthy MDMs as determined by extracellular flux. Data are shown as mean ± SEM. Each dot represents the average of an experimental duplicate of one donor (A) or the average of an experimental quadruplicate of one donor (B) (n = 4 (A) or 3 (B) healthy donors). *$P < 0.05$ or **$P < 0.01$ by one-way ANOVA with Sidak's correction for multiple comparisons (A) or by unpaired two-tailed t-test (B).

cytokine levels, in plasma samples from adult lcFAOD patients in a non-stressed outpatient setting.

The difference between Vallejo et al. in comparison to McCoin et al. and our study, might be attributed to the younger age of the Vallejo cohort and a shift from general metabolic decompensations with multi-organ involvement to mainly muscle symptoms or rhabdomyolysis, where rhabdomyolysis is observed in many lcFAOD patients as they age [32]. Additionally, both the McCoin study and ours carefully matched control subjects for age and sex, factors known to influence inflammation [33]. However, despite this matching, the body mass index (BMI) of patients in our study was slightly higher than the BMI of the control subjects, an aspect that may also attribute to enhanced systemic cytokine signaling [34]. Lastly, our inclusion of only adult patients with differing lcFAOD, may have resulted in including milder phenotypes compared to the McCoin study. As such, disease severity may vary greatly among different cohorts and focusing on individual defects may provide more insight on the specific mechanisms behind these results [35]. Together, we did not observe major signs of inflammation, nor grossly altered macrophage response to inflammatory stimuli, in adult patients with lcFAODs in a stable, well controlled situation. This suggests that, at least for the adult lcFAOD patients and based on our readouts, there is no rationale for anti-inflammatory therapy as was suggested in a previous publication [5]. Together with previous findings, our results underscore the diverse functional outcomes observed in lcFAOD, and emphasizing the importance of further investigation.

Macrophages stimulated with LPS or IL-4 rewire FA metabolism [8,36], highlighting the importance of this metabolic pathway in macrophage activation states. Concomitantly, recent work revealed that severe but not mild lcFAOD results in the downregulation of LPS-receptor toll-like receptor 4 (TLR4) and subsequent ablated LPS responses *in vitro* [37]. In line with this, our study revealed no effect of si*ACADVL* or lcFAOD on LPS responses in whole blood *ex vivo* or in *in vitro* macrophages, suggesting non-severe FAOD in our patient cohort. Additionally, this reveals that intervening in FAO does not affect the inflammatory LPS responses in blood leukocytes and macrophages.

Alternative activation of human macrophages with IL-4 is generally characterized by an increased flux through FAO and the upregulation of specific activation markers [10,12]. Treatment with relevant concentrations of CPT1-inhibitor etomoxir does not impact IL-4-induced macrophage polarization [10,11,38,39]. Interestingly, in our study, lcFAOD and si*ACADVL* macrophages displayed an augmentation in IL-4-induced CD206 expression, along with enhanced CD206 levels on non-classical monocytes from lcFAOD patients. The mannose receptor (CD206) is generally involved in macrophage maturation [40] and is upregulated by IL-4 to increase the uptake of mannosylated ligands and lipids derived from membranes of apoptotic cells [41,42]. CD206 is considered to be mainly involved in the resolution of inflammation, as macrophages with higher CD206 expression are more abundant in rheumatoid arthritis patients in disease remission than in active disease [43]. In line with these seemingly protective effects of CD206, the other marker that was upregulated in IL-4-induced lcFAOD macrophages but not si*ACADVL* macrophages, CD200R, is also involved in immune suppression and hereby supports resolution of inflammation [44]. The upregulation of resolution-associated surface proteins CD206 and CD200R suggests that macrophages derived from lcFAOD patients are better capable of resolving inflammation *in vitro* without altering the response to LPS. Additionally, the absence of the upregulation of CD200R in si*ACADVL* macrophages indicates a possible compensation mechanism for long-term lcFAO ablation. Furthermore, since the effects of enhanced CD206 levels in lcFAOD patients *in vivo* are not completely clear future studies should decipher what the implications are of this finding for organs where $CD206^{+}$ macrophages play major roles like the lungs [45] or adipose tissue [46] in either material from mouse models or from human biopsies.

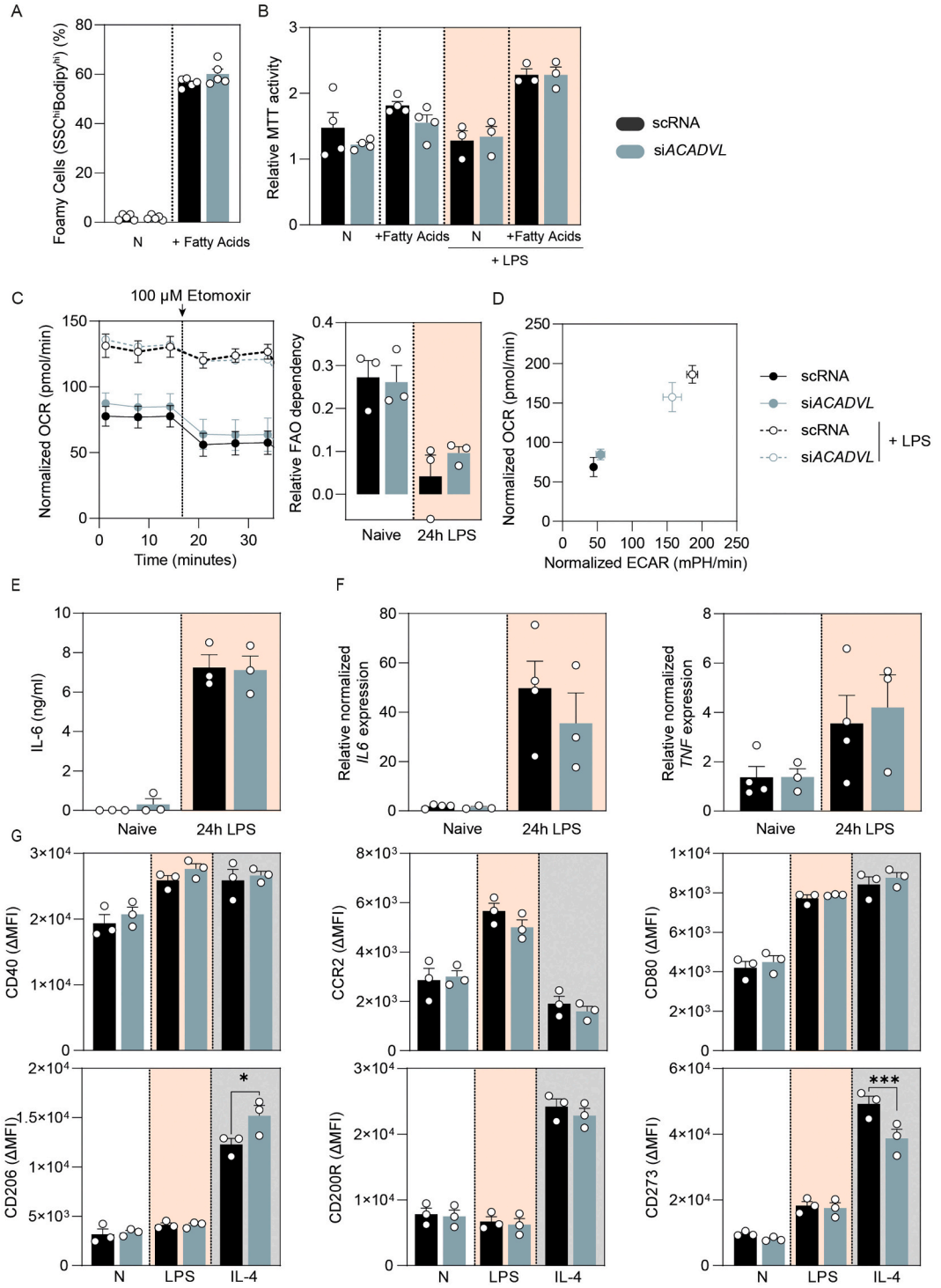

Fig. 3. Human macrophages with siRNA-mediated *ACADVL* knockdown remain their lipid handling capacities but alter IL-4-induced cell activation. A) Foam cell formation after exposure to lcFA-enriched medium as determined by BODIPY493/503 with flow cytometry. B) MTT activity in naïve and LPS-stimulated macrophages exposed to normal or lcFA-enriched medium. C) Relative OCR dependent on FAO in naïve and LPS-stimulated macrophages with and without *ACADVL* KD. D) Basal normalized OCR and ECAR in naïve and LPS-stimulated macrophages with and without *ACADVL* KD. E) IL-6 secretion from scRNA and *ACADVL* KD macrophages upon 24 h activation with LPS. F) Activation marker expression in response to LPS and IL-4 in scRNA and si*ACADVL* KD macrophages as determined by flow cytometry. Data are shown as mean ± SEM. Each dot represents the average value of triplicates of one donor ($n = 5$ (A), 3–4 (B) or 3 (C-F). $^{*}P < 0.05$ or $^{***}P < 0.001$ by one-way ANOVA with Sidak's correction for multiple comparisons.

Previously, we demonstrated that prolonged genetic depletion of metabolic genes may rewire metabolism, with cells utilizing alternative fuels to meet their cellular demands [29]. Intriguingly, studies in VLCAD-deficient mice have shown metabolic rewiring in key organs, such as the liver, the heart and skeletal muscles [47], which are among the most affected organs in lcFAOD patients [48]. Furthermore, VLCAD-deficient mice show alterations in citric acid cycle-metabolites like succinate [49], which can also influence immune cell function as a so-called immunometabolite [50]. However, the effects on immunological parameters in VLCAD-deficient mice remain relatively unexplored

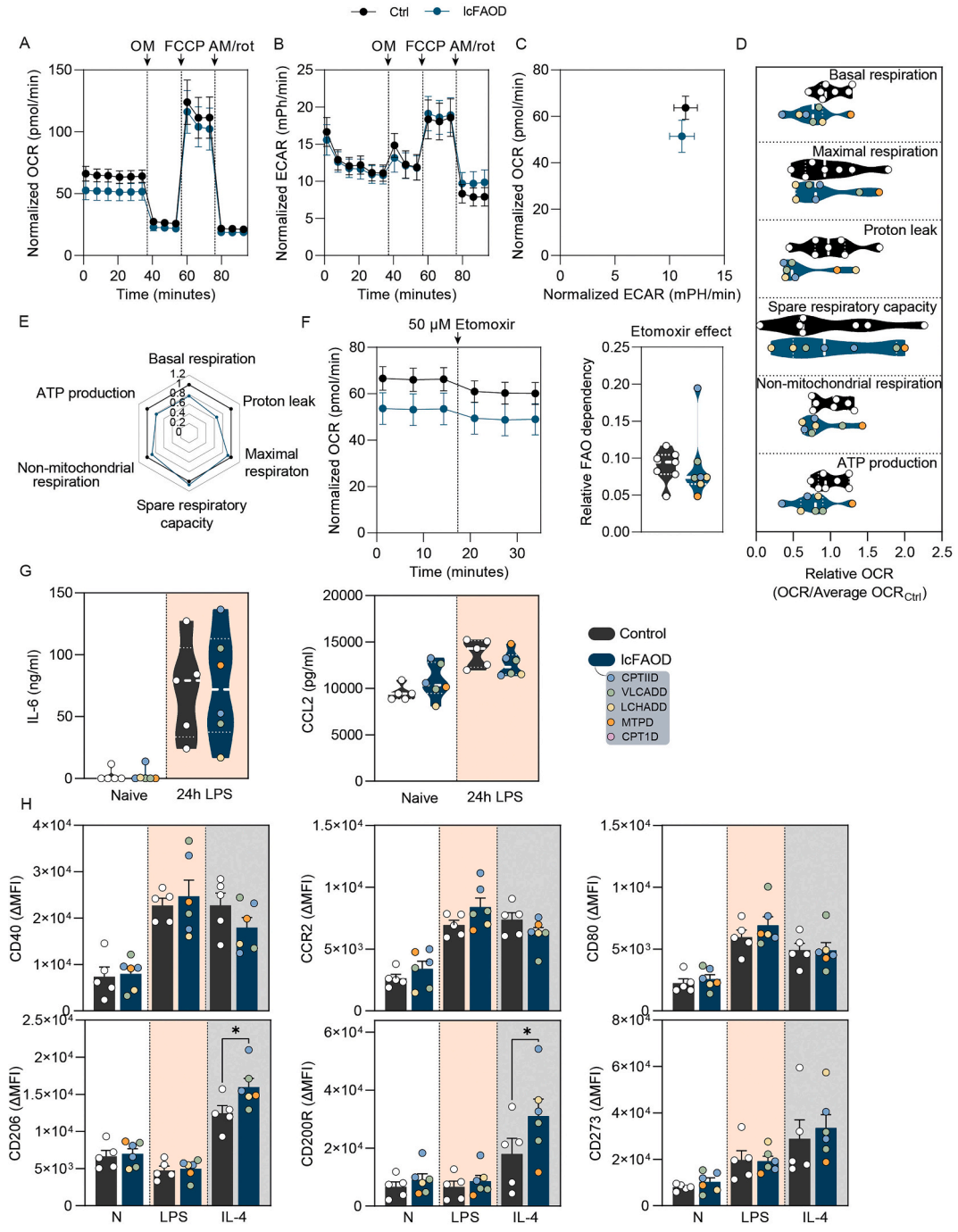

Fig. 4. Control and lcFAOD-patient monocyte-derived macrophages are metabolically similar but evoke enhanced responses to IL-4. A, B) Normalized OCR (A) and ECAR (B) of control and patient macrophages in a mitostress test as measured by extracellular flux. C) Basal normalized OCR and ECAR levels in control and patient macrophages. D, E) Relative extracellular flux parameters in control and patient macrophages. F) Relative OCR dependent on FAO in control and patient macrophages as determined by extracellular flux. G, H) Secretion of IL-6 (G) and CCL2 (H) from LPS-activated control- and patient-macrophages. I) Activation marker expression in response to LPS and IL-4 in control and patient macrophages as determined by flow cytometry. Data are presented as mean ± SEM (A-C, F1, H) or as median and quartiles (D, F2, G). Each dot represents the average value of triplicates (A) or duplicates (G-H) per control or patient ($n = 5$ controls, $n = 6$ patients). *$P < 0.05$ by one-way ANOVA with Sidak's correction for multiple comparisons.

but could offer valuable insights into metabolic rewiring in macrophages following genetic *Acadvl* depletion. In our study, we did not observe clear metabolic rewiring in human lcFAOD macrophages in basal metabolic pathways *in vitro*. Therefore, other pathways warrant further investigation, such as transcriptomics analysis on blood leukocytes or macrophages derived from induced pluripotent stem cells (iPSCs) lcFAOD.

While our study provides important insights in monocyte profiles and macrophage function in patients with inherited lcFAODs, we acknowledge that our research comes with some limitations. First, although similar to other papers in the field, the number of recruited patients was relatively small. Thereby, a lack of statistical power limits drawing definitive conclusions. Despite that lcFAODs are rare disorders and recruiting large numbers of age- and sex-matched patients is a significant challenge, we managed to recruit patients with a relatively similar age (33.9 ± 3.4 years), limiting age as a covariate and

strengthening conclusions for this age group. Second, the analyses on circulating monocytes included a selective set of 12 surface markers, and a small panel of cytokines was used to determine the LPS-induced inflammatory response in whole blood. In the current -omics era, more unbiased and comprehensive approaches are feasible, and future studies may employ broader analyses that encompass a wider range of markers to phenotype all immune cells.

Altogether, our data provide a novel insight into human macrophage functioning upon lcFAO-deficiency and show a more reparative phenotype. Yet, further research with greater statistical power and comprehensive metabolic and inflammatory analyses, including *in vivo* data, is warranted. This study provides the fundament for future investigations along this avenue.

4. Material and methods

4.1. Patient inclusion, study design, and blood collection

Human research protocols were approved by the Amsterdam UMC Academic Medical Center Medical Ethical Committee and in accordance with the declaration of Helsinki. Patients with lcFAO disorders were recruited during their visits to the hospital after receiving an information letter. lcFAOD were confirmed by genotype for all and enzyme activity for most patients (Table 1). In accordance with the study protocol (nr. NL67564.018.18), samples were taken by venipuncture combined with samples taken for regular care between September 2020 and October 2023. Blood from healthy volunteers was taken around the same time, and volunteers were recruited in accordance with study protocol nr. 2015_074. The need for ethical approval was waived. Prior to sample donation, all donors gave informed consent. Exclusion criteria were diabetes mellitus, BMI $>$ 30 kg/m^2 and/or regular use of inflammation-modulating drugs *e.g.* NSAIDs, HMG-CoA-reductase inhibitors (also known as statins) or (inhalation) corticosteroids.

On the day of inclusion, 30 ml blood was collected in K3EDTA BD Vacutainer (BD Biosciences) tubes from the patient and a sex- and age-matched healthy control (±10y) (Table 1). Blood from all tubes of the same donor was combined. 1 ml blood was taken for flow cytometry analysis. Plasma was collected by 7-min 300 *g* centrifugation at room temperature (RT) of 5 ml blood and stored at −80 °C in aliquots. The cell pellet obtained after plasma collection and the remaining part of whole blood was used for PBMC isolation.

4.2. Whole blood flow cytometry

Whole blood flow cytometric analysis was performed by lysing 1 ml blood in 9 ml 1× RBC lysis buffer (eBioscience) for 12 min at RT. The reaction was stopped by topping up with FACS buffer (PBS + 0.5 % BSA + 0.02 % sodium azide (Sigma)) and centrifugation for 6 min at 1500 rpm. Supernatant was removed and cells were resuspended in 1 ml RBC lysis buffer for additional lysis of 5 min at RT. The reaction was again stopped by topping up with FACS buffer and washing twice in FACS buffer by 6-min centrifugation at 1500 rpm at RT. Cells were divided into a V-bottom plate for samples and FMO controls and incubated for 15 min with 1:1000 Fixable Viability Dye e780 (eBioscience) and 1:200 blocking antibodies (BD) in 50 μl PBS. Subsequently, cells were washed with FACS buffer during 5-min centrifugation at 1600 rpm at 4 °C and stained in 25 μl antibody cocktail in FACS buffer on ice for 30 min. Antibodies were used in the dilutions specified in Supplementary Table 1. Lastly, cells were washed with PBS and fixed in 1.6 % PFA (Electron Microscopy Sciences) for 15 min on ice, washed and resuspended in FACS buffer until acquisition. Acquisition was performed within 24 h after fixation on an LSR Fortessa (BD). Data was analyzed using FlowJo (10.7.2) and presented as median fluorescent intensity $(MFI)_{sample}$-$(MFI)_{FMO}$.

4.3. Whole blood LPS challenge

Fresh blood was diluted 1/5 in plain RPMI (Gibco) medium in 24-well plates and treated for 24 h with 100 ng/ml LPS (Sigma, L2637). Subsequently, medium was collected and centrifuged for 5 min at 20,000 g at room temperature. Supernatants were collected and stored in aliquots at −80 °C until subsequent analysis.

4.4. PBMC isolation

Peripheral blood mononuclear cells (PBMCs) were isolated with a Ficoll-gradient. Briefly, blood was diluted 1:1 with PBS-1 % Citrate and 30 ml diluted blood was gently added on top of 15 ml Ficoll in a 50 ml tube. Tubes were centrifuged at 2000 *g* for 30 min at RT without breaks after which the interphase was collected and washed twice with PBS-1% citrate. Then, cells were frozen in 90 % FCS and 10 % DMSO in a freezing container (Nalgene) for storage in liquid nitrogen until further use.

4.5. Cytokine ELISA and CBA

CBA analysis was performed according to manufacturer's protocol (Biolegend Multiplex).

Cytokine secretion (IL-6, TNF, CCL2) in whole blood LPS challenge samples and cell supernatants was quantified using ELISA (Uncoated ELISA kit, Invitrogen), according to manufacturer's protocols.

4.6. Monocyte isolation and HMDM culture from buffy coats

Buffy coats were obtained from Sanquin blood bank (Amsterdam, Netherlands). PBMCs were isolated with a Ficoll/Lymphoprep gradient (Greiner Biosciences) and careful centrifugation at 800 *g* for 30 min with lowest deceleration. Next, monocytes were isolated by applying 120–150*10^6 cells on top of a 46 % Percoll™ (Cytiva) solution followed by careful centrifugation at 2000 rpm for 20 min. Monocytes were counted and plated at a density of 2*10^6 cells/ml in the appropriate plates for each experiment in IMDM medium containing HEPES (Gibco) supplemented with 2 mM L-glutamine without antibiotics (full IMDM medium), and containing 1 % FCS. After settling for 1 h, medium was replaced with full IMDM medium with 10 % FCS and 50 ng/ml M-CSF (Miltenyi) for 6-day differentiation. On day 3, medium was replaced with fresh medium supplemented with M-CSF. On day 6, cells were treated with 100 ng/ml LPS or 20 ng/ml human recombinantIL-4 (Peprotech, 300–02) or with scRNA control or siRNA-knockdown.

4.7. siRNA-mediated knockdown of VLCAD

Knockdown of *ACADVL* was performed using ON-TARGETplus siRNA-SMARTpool (Dharmacon) on differentiated primary hMDMs in antibiotic free medium. VLCAD was targeted by ON-TARGETplus Human *ACADVL* (37) siRNA SMARTpool (Dharmacon) and controlled by scRNA of ON-TARGETplus Non-targeting Pool (Dharmacon). First, siRNA and scRNA stocks of 5 μM in RNAse-free sterile H_2O were diluted to 250 nM in blank IMDM medium and incubated for 5 min at RT. DharmaFECT Transfection reagent 4 was diluted 1/100 in blank IMDM medium and added 1:1 to 250 nM siRNA/scRNA and subsequently incubated for 20 min at RT. Mixed scRNA/siRNA and transfection reagent were then diluted 1/5 with full IMDM with 50 ng/ml M-CSF and incubated with cultured cells for 18 h. Cells then rested for 24 h in antibiotic-free IMDM with 50 ng/ml and subsequently stimulated for experiments with 100 ng/ml LPS, 20 ng/ml IL-4, or with a 0.6 mM mixture of oleic acid:palmitic acid (Sigma) 1:2.

4.8. Gene expression analysis

For gene expression analysis, macrophages were cultured in 24-well plates (1*10^6 cells/ml) as described before. RNA was isolated using the

GeneJet RNA Purification kit (ThermoFisher) according to manufacturer's protocol from $5*10^5$ cultured cells. Subsequently, cDNA was synthesized from 400 ng total RNA using the High-Capacity cDNA Reverse Transcription kit (ThermoFisher). RNA was quantified using qPCR with SYBR Green Fast mix (Applied Biosystems) on a ViiA7 system (Applied Biosystems). Expression levels were normalized to the expression levels of housekeeping genes *GNB2L1* and *PPIA*. Primer sequences are listed in Supplementary Table 2.

4.9. Immunoblotting

hMDMs were cultured as $2*10^6$ cells in 6-well plates. Protein was harvested by washing cells with cold PBS and subsequent 15-min incubation with RIPA buffer supplemented with fresh protease inhibitor cocktail (Sigma-Aldrich). Lysates were scraped from the wells and centrifuged at 2000 *g* for 10 min at 4 °C. Protein concentration was determined with a DC assay (Bio-Rad) according to manufacturer's protocol. Sample protein concentrations were equalized with MilliQ and 4× Laemmli loading buffer (Bio-Rad) supplemented with β-mercapthoethanol and subsequently heated for 10 min at 95 °C for denaturation. Of each sample, a final amount of 28.8 μg protein was loaded on a 10 % running gel and after gel electrophoresis semi-dry transferred to a 0.2 μm nitrocellulose Trans-Blot membrane (Bio-Rad) with a Trans-Blot turbo system (Bio-Rad). Blots were blocked by TBS Blocking buffer (Odyssey) for 1 h and left overnight with 1:1000 anti-ACADVL (Sigma-Aldrich) antibody in TBS blocking buffer at 4 °C. Next day, blots were incubated with 1:15000 secondary goat anti-rabbit 800 (Odyssey) for 1 h, then 1:5000 β-actin (Sigma-Aldrich) for 1 h followed by 1 h 1:15000 goat anti-mouse 480 (Odyssey), all at RT. Blots were imaged with a Sapphire Biomolecular Imager (Azure Biosystems) and quantified using ImageJ/Fiji (1.8.0).

4.10. $CD14^+$-monocyte isolation from frozen PBMCs

Patient and control monocytes from frozen PBMCs were isolated using $CD14^+$-positive selection beads (Miltenyi). Cells were quickly defrosted, added to 10 ml blank IMDM (Gibco) medium and centrifuged at 300 *g* for 7 min. Cells were counted and resuspended in 80 μl MACS buffer (PBS + 0.5 % BSA + 2 mM EDTA). Cells were incubated with 20 μl of CD14 microbeads at 4 °C for 15 min. Cells were washed with MACS buffer and centrifugation at 300 *g* for 7 min and subsequently resuspended in 500 μl MACS buffer. LS columns were placed on MidiMACS magnets and rinsed with 3 ml MACS buffer. Next, cell suspension was added and unlabeled cells were collected. Columns were washed 3 times with 3 ml MACS buffer and then placed over a collection tube. Cells were collected by firmly pushing the plunger into the column detached from the magnet. $CD14^+$-monocytes were counted and diluted and plated as $1*10^6$ cells/ml in full IMDM medium with 100 U/ml penicillin and 100 μg/ml streptomycin and containing 10 % FCS and 50 ng/ml M-CSF (Miltenyi). Differentiation was done in 96-well plates for 6 days with intermediate medium replacement on day 3. On day 6, cells were stimulated for subsequent analyses.

4.11. Extracellular flux analysis

OCR and ECAR rates were determined by extracellular flux analysis using the Seahorse XFe-96 Flux Analyzer (Agilent) as described previously [27,51]. Briefly, cells were plated at a density of $7.5*10^4$ cells per well in 75 μl culture medium. 1 h prior to the assay, medium was replaced by Seahorse base medium (Sigma Aldrich) supplemented with 25 mM Glucose, 5 mM HEPES and 2 mM L-glutamine. The run consisted of 4 injections and followed by 2 min of mixing and 3 min measuring. The first injection was either blank medium or 50 μM or 100 μM etomoxir (Selleckchem) followed by the injection of oligomycin (final concentration 1.5 μM), FCCP (final concentration 1.5 μM) and lastly an injection of antimycin A (final concentration 2.5 μM) with rotenone (final concentration 1.5 μM) and Hoechst 33342 (ThermoFisher) (final concentration 5 μg/ml). After finishing the run, Hoechst signal was imaged on a Cytation 5 Cell Imaging multi-mode reader (BioTek) with 4× magnification and a 365 nm LED and a EX377/50 EM477/60 filter cube. Data was normalized for cell count as follows:

$$\text{Normalized OCR or ECAR} = \text{OCR or ECAR} \Big/ \frac{\text{cell count in center of well}}{\text{average of plate}}$$

Data were analyzed using Wave software version 2.6.0.31.

4.12. Flow cytometry on cultured macrophages

Flow cytometry on cultured macrophages was performed by culturing $1*10^5$ cells per well in 96-well plates. Cells were harvested by incubating for 10 min in ice-cold 0.5 mM EDTA and subsequent gently resuspending cells by pipetting. Cells were moved to a V-bottom plate, and incubated for 15 min with 1:1000 Fixable Viability Dye e780 (eBioscience) and 1:200 Fc block (BD) in 50 μl PBS. Subsequently, cells were washed with FACS buffer during 5-min centrifugation at 1600 rpm at 4 °C and stained in 25 μl antibody cocktail in FACS buffer on ice for 30 min. Antibodies were used in the dilutions as indicated in Supplementary Table 1. Lastly, cells were washed with PBS and fixed in 1.6 % PFA for 15 min on ice, washed and resuspended in FACS buffer until acquisition. Acquisition was performed within 24 h after fixation on an LSR Fortessa (BD). Data was analyzed using FlowJo (10.7.2) and presented as median fluorescent intensity $(MFI)_{sample}$-$(MFI)_{unstained}$.

4.13. Statistical analysis

Data are presented as mean ± standard error of the mean (SEM) unless specified differently. Normal distribution was tested using the Shapiro-Wilk test for normality in GraphPad Prism software (10.2.0). Statistical significance was analyzed using a two-tailed student's *t*-test or an ordinary one-way ANOVA followed by Sidak's correction for multiple comparisons with GraphPad Prism. *P* values <0.05 were considered statistically significant indicated by $*p < 0.05$, $**p < 0.01$, $***p < 0.001$.

Funding

J.V.D.B. received a Netherlands Hearth Foundation senior fellowhip (2017T048), an Enw-klein-1 grant from NOW (OCENW.KLEIN.268) and a consortia grant from European Research Area network on Cardiovascular Diseases (ERA-CVD 2019T108).

Declaration of generative AI-assisted technologies

During the preparation of this work the authors used ChatGPT in the last phases of manuscript writing to improve language and enhance readability. After using this tool/service, the authors reviewed and edited the content as needed and take full responsibility for the content of the publication.

CRediT authorship contribution statement

Sanne G.S. Verberk: Writing – review & editing, Writing – original draft, Visualization, Project administration, Methodology, Investigation, Formal analysis, Data curation, Conceptualization. **Nico Hahn:** Investigation, Formal analysis. **Daan Heister:** Project administration, Investigation, Formal analysis. **Jorien Haverkamp:** Project administration, Data curation. **Khya S. Snelder:** Formal analysis, Data curation. **Kyra E. de Goede:** Writing – review & editing, Methodology, Investigation. **Friederieke S. Gorki:** Methodology, Investigation. **Jerome J.A. Hendriks:** Writing – review & editing. **Riekelt H. Houtkooper:** Writing – review & editing. **Gepke Visser:** Writing – review & editing. **Barbara Sjouke:** Writing – review & editing, Supervision, Project administration,

Methodology, Conceptualization. **Mirjam Langeveld:** Writing – review & editing, Supervision, Resources, Project administration. **Jan Van den Bossche:** Writing – review & editing, Supervision, Resources, Funding acquisition, Conceptualization.

Declaration of competing interest

All authors declare no competing interests.

Data availability

Data will be made available on request.

Acknowledgements

We thank all patients and healthy controls for contributing to this study. Additionally, we thank Cora Chadick for training and assisting in setting up the flow cytometry panel, Jasper Koning for his help with performing the multiplex cytokine measurements, and Myrthe den Toom and Tanja Konijn for drawing blood from healthy controls.

Appendix A. Supplementary data

Supplementary data to this article can be found online at https://doi.org/10.1016/j.bbadis.2024.167524.

References

[1] G. Elizondo, et al., Effects of fasting, feeding and exercise on plasma acylcarnitines among subjects with CPT2D, VLCADD and LCHADD/TFPD, Mol. Genet. Metab. 131 (2020) 90–97, https://doi.org/10.1016/j.ymgme.2020.09.001.
[2] S.J.G. Knottnerus, et al., Disorders of mitochondrial long-chain fatty acid oxidation and the carnitine shuttle, Rev. Endocr. Metab. Disord. 19 (2018) 93–106, https://doi.org/10.1007/s11154-018-9448-1.
[3] S.C. Grunert, et al., The spectrum of peripheral neuropathy in disorders of the mitochondrial trifunctional protein, J. Inherit. Metab. Dis. 44 (2021) 893–902, https://doi.org/10.1002/jimd.12372.
[4] R. Williams-Hall, et al., Qualitative evaluation of the symptoms and quality of life impacts of long-chain fatty acid oxidation disorders, Ther. Adv. Endocrinol. Metab. 13 (2022), https://doi.org/10.1177/20420188211065655, 20420188211065655.
[5] A.N. Vallejo, et al., Pervasive inflammatory activation in patients with deficiency in very-long-chain acyl-coA dehydrogenase (VLCADD), Clin Transl Immunology 10 (2021) e1304, https://doi.org/10.1002/cti2.1304.
[6] C.S. McCoin, et al., Blood cytokine patterns suggest a modest inflammation phenotype in subjects with long-chain fatty acid oxidation disorders, Physiol. Rep. 7 (2019) e14037. 10.14814/phy2.14037.
[7] J.M. Rutkowsky, et al., Acylcarnitines activate proinflammatory signaling pathways, Am. J. Physiol. Endocrinol. Metab. 306 (2014) E1378–E1387, https://doi.org/10.1152/ajpendo.00656.2013.
[8] A.K. Jha, et al., Network integration of parallel metabolic and transcriptional data reveals metabolic modules that regulate macrophage polarization, Immunity 42 (2015) 419–430, https://doi.org/10.1016/j.immuni.2015.02.005.
[9] L.A. O'Neill, et al., A guide to immunometabolism for immunologists, Nat. Rev. Immunol. 16 (2016) 553–565, https://doi.org/10.1038/nri.2016.70.
[10] J. Van den Bossche, et al., Mitochondrial dysfunction prevents repolarization of inflammatory macrophages, Cell Rep. 17 (2016) 684–696, https://doi.org/10.1016/j.celrep.2016.09.008.
[11] D. Namgaladze, B. Brune, Fatty acid oxidation is dispensable for human macrophage IL-4-induced polarization, Biochim. Biophys. Acta 1841 (2014) 1329–1335, https://doi.org/10.1016/j.bbalip.2014.06.007.
[12] D. Vats, et al., Oxidative metabolism and PGC-1beta attenuate macrophage-mediated inflammation, Cell Metab. 4 (2006) 13–24, https://doi.org/10.1016/j.cmet.2006.05.011.
[13] M. Nomura, et al., Fatty acid oxidation in macrophage polarization, Nat. Immunol. 17 (2016) 216–217, https://doi.org/10.1038/ni.3366.
[14] J. Van den Bossche, G.J.W. van der Windt, Fatty acid oxidation in macrophages and T cells: time for reassessment? Cell Metab. 28 (2018) 538–540, https://doi.org/10.1016/j.cmet.2018.09.018.
[15] N. Raulien, et al., Fatty acid oxidation compensates for lipopolysaccharide-induced Warburg effect in glucose-deprived monocytes, Front. Immunol. 8 (2017) 609, https://doi.org/10.3389/fimmu.2017.00609.
[16] J. Van den Bossche, et al., Macrophage Immunometabolism: where are we (going)? Trends Immunol. 38 (2017) 395–406, https://doi.org/10.1016/j.it.2017.03.001.
[17] J.S. Moon, et al., NOX4-dependent fatty acid oxidation promotes NLRP3 inflammasome activation in macrophages, Nat. Med. 22 (2016) 1002–1012, https://doi.org/10.1038/nm.4153.
[18] R. Zhou, et al., A role for mitochondria in NLRP3 inflammasome activation, Nature 469 (2011) 221–225, https://doi.org/10.1038/nature09663.
[19] P.J. Hohensinner, et al., Pharmacological inhibition of fatty acid oxidation reduces atherosclerosis progression by suppression of macrophage NLRP3 inflammasome activation, Biochem. Pharmacol. 190 (2021) 114634, https://doi.org/10.1016/j.bcp.2021.114634.
[20] M. Nomura, et al., Macrophage fatty acid oxidation inhibits atherosclerosis progression, J. Mol. Cell. Cardiol. 127 (2019) 270–276, https://doi.org/10.1016/j.yjmcc.2019.01.003.
[21] M. Yuasa, et al., Evaluation of metabolic defects in fatty acid oxidation using peripheral blood mononuclear cells loaded with deuterium-labeled fatty acids, Dis. Markers 2019 (2019) 2984747, https://doi.org/10.1155/2019/2984747.
[22] G.D. Thomas, et al., Human blood monocyte subsets: a new gating strategy defined using cell surface markers identified by mass cytometry, Arterioscler. Thromb. Vasc. Biol. 37 (2017) 1548–1558, https://doi.org/10.1161/ATVBAHA.117.309145.
[23] R.D. Abeles, et al., CD14, CD16 and HLA-DR reliably identifies human monocytes and their subsets in the context of pathologically reduced HLA-DR expression by CD14(hi) /CD16(neg) monocytes: expansion of CD14(hi) /CD16(pos) and contraction of CD14(lo) /CD16(pos) monocytes in acute liver failure, Cytometry A 81 (2012) 823–834, https://doi.org/10.1002/cyto.a.22104.
[24] M.C. Peters, et al., Plasma interleukin-6 concentrations, metabolic dysfunction, and asthma severity: a cross-sectional analysis of two cohorts, Lancet Respir. Med. 4 (2016) 574–584, https://doi.org/10.1016/S2213-2600(16)30048-0.
[25] D.K. Thompson, et al., Critical appraisal of four IL-6 immunoassays, PloS One 7 (2012) e30659, https://doi.org/10.1371/journal.pone.0030659.
[26] A. Mahittikorn, et al., Elevation of serum interleukin-1beta levels as a potential indicator for malarial infection and severe malaria: a meta-analysis, Malar. J. 21 (2022) 308, https://doi.org/10.1186/s12936-022-04325-0.
[27] S.G.S. Verberk, et al., An integrated toolbox to profile macrophage immunometabolism, Cell Rep Methods 2 (2022) 100192, https://doi.org/10.1016/j.crmeth.2022.100192.
[28] M. Genoula, et al., Fatty acid oxidation of alternatively activated macrophages prevents foam cell formation, but mycobacterium tuberculosis counteracts this process via HIF-1alpha activation, PLoS Pathog. 16 (2020) e1008929, https://doi.org/10.1371/journal.ppat.1008929.
[29] J. Baardman, et al., Macrophage ATP citrate lyase deficiency stabilizes atherosclerotic plaques, Nat. Commun. 11 (2020) 6296, https://doi.org/10.1038/s41467-020-20141-z.
[30] S.G.S. Verberk, et al., Myeloid ATP citrate Lyase regulates macrophage inflammatory responses in vitro without altering inflammatory disease outcomes, Front. Immunol. 12 (2021) 669920, https://doi.org/10.3389/fimmu.2021.669920.
[31] E. Gonzalez-Hurtado, et al., Loss of macrophage fatty acid oxidation does not potentiate systemic metabolic dysfunction, Am. J. Physiol. Endocrinol. Metab. 312 (2017) E381–E393, https://doi.org/10.1152/ajpendo.00408.2016.
[32] A. Rouyer, et al., Long-term prognosis of fatty-acid oxidation disorders in adults: optimism despite the limited effective therapies available, Eur. J. Neurol. 31 (2024) e16138, https://doi.org/10.1111/ene.16138.
[33] F. Olivieri, et al., Sex/gender-related differences in inflammaging, Mech. Ageing Dev. 211 (2023) 111792, https://doi.org/10.1016/j.mad.2023.111792.
[34] I.B. Kosovski, et al., Exploring the link between inflammatory biomarkers and Adipometrics in healthy young adults aged 20-35 years, Nutrients 16 (2024), https://doi.org/10.3390/nu16020257.
[35] U. Spiekerkoetter, Mitochondrial fatty acid oxidation disorders: clinical presentation of long-chain fatty acid oxidation defects before and after newborn screening, J. Inherit. Metab. Dis. 33 (2010) 527–532, https://doi.org/10.1007/s10545-010-9090-x.
[36] R. Li, et al., Mitochondrial STAT3 exacerbates LPS-induced sepsis by driving CPT1a-mediated fatty acid oxidation, Theranostics 12 (2022) 976–998, https://doi.org/10.7150/thno.63751.
[37] S. Mosegaard, et al., Human inborn errors of long-chain fatty acid oxidation show impaired inflammatory responses to TLR4-ligand LPS, bioRxiv (2023), https://doi.org/10.1101/2023.08.30.555512, 2023.2008.2030.555512.
[38] A.S. Divakaruni, et al., Etomoxir inhibits macrophage polarization by disrupting CoA homeostasis, Cell Metab. 28 (490–503) (2018) e497, https://doi.org/10.1016/j.cmet.2018.06.001.
[39] Z. Tan, et al., Pyruvate dehydrogenase kinase 1 participates in macrophage polarization via regulating glucose metabolism, J. Immunol. 194 (2015) 6082–6089, https://doi.org/10.4049/jimmunol.1402469.
[40] P.B. Wright, et al., The mannose receptor (CD206) identifies a population of colonic macrophages in health and inflammatory bowel disease, Sci. Rep. 11 (2021) 19616, https://doi.org/10.1038/s41598-021-98611-7.
[41] M. Stein, et al., Interleukin 4 potently enhances murine macrophage mannose receptor activity: a marker of alternative immunologic macrophage activation, J. Exp. Med. 176 (1992) 287–292, https://doi.org/10.1084/jem.176.1.287.
[42] A. Vogel, et al., Lipid scavenging macrophages and inflammation, Biochim. Biophys. Acta Mol. Cell Biol. Lipids 1867 (2022) 159066, https://doi.org/10.1016/j.bbalip.2021.159066.
[43] S. Alivernini, et al., Distinct synovial tissue macrophage subsets regulate inflammation and remission in rheumatoid arthritis, Nat. Med. 26 (2020) 1295–1306, https://doi.org/10.1038/s41591-020-0939-8.
[44] M.C. Jenmalm, et al., Regulation of myeloid cell function through the CD200 receptor, J. Immunol. 176 (2006) 191–199, https://doi.org/10.4049/jimmunol.176.1.191.

[45] E. Mitsi, et al., Human alveolar macrophages predominately express combined classical M1 and M2 surface markers in steady state, Respir. Res. 19 (2018) 66, https://doi.org/10.1186/s12931-018-0777-0.
[46] A. Nawaz, et al., CD206(+) M2-like macrophages regulate systemic glucose metabolism by inhibiting proliferation of adipocyte progenitors, Nat. Commun. 8 (2017) 286, https://doi.org/10.1038/s41467-017-00231-1.
[47] S. Tucci, et al., Tissue-specific strategies of the very-long chain acyl-CoA dehydrogenase-deficient (VLCAD−/−) mouse to compensate a defective fatty acid beta-oxidation, PloS One 7 (2012) e45429, https://doi.org/10.1371/journal.pone.0045429.
[48] S.J.G. Knottnerus, et al., Electrophysiological abnormalities in VLCAD deficient hiPSC-cardiomyocytes can be improved by lowering accumulation of fatty acid oxidation intermediates, Int. J. Mol. Sci. 21 (2020), https://doi.org/10.3390/ijms21072589.
[49] G. Gaston, et al., Cardiac tissue citric acid cycle intermediates in exercised very long-chain acyl-CoA dehydrogenase-deficient mice fed triheptanoin or medium-chain triglyceride, J. Inherit. Metab. Dis. 43 (2020) 1232–1242, https://doi.org/10.1002/jimd.12284.
[50] K.J. Harber, et al., Succinate is an inflammation-induced Immunoregulatory metabolite in macrophages, Metabolites 10 (2020), https://doi.org/10.3390/metabo10090372.
[51] J. Van den Bossche, et al., Metabolic characterization of polarized M1 and M2 bone marrow-derived macrophages using real-time extracellular flux analysis, JoVE (Journal of Visualized Experiments) (105) (Nov 28, 2015) 53424, https://doi.org/10.3791/53424.